AIAA JOURNAL
Vol. 35, No. 1, January 1997

Effects of Longitudinal and Hoop Stiffeners on Damage Propagation in Pressurized Composite Cylinders

Haryanto T. Budiman,* Kerry F. Henault,† and Paul A. Lagace‡
Massachusetts Institute of Technology, Cambridge, Massachusetts 02139

An experimental study was conducted on the combined effects of longitudinal and hoop stiffening bands on the damage propagation in pressurized composite cylindrical shells. Damage was simulated as through-thickness longitudinal slits. Two different stiffener configurations were studied: 1) alternating continuous and broken hoop and longitudinal stiffeners (type A) and 2) continuous longitudinal and hoop fabric stiffeners (type B). In all but one cylinder, damage turned 90 deg near the edge of the hoop stiffening bands. In cases in which damage turned, it continued its propagation in the hoop direction, breaking the first set of longitudinal reinforcement layers, inducing secondary damage modes (such as stiffener debonding and delamination) along the way, and generally being arrested at the second set of longitudinal stiffeners. Damage redirection by the first set of longitudinal stiffeners was seen in one cylinder that had significant reinforcement in the longitudinal direction. The longitudinal stiffeners are, therefore, not as effective as the hoop stiffeners in inducing damage redirection in the laboratory-scaled specimens tested. The difference in the stiffener curvature and the presence of significant bending due to the flapping phenomenon caused by internal pressure during rupture contribute to this observed phenomenon. Since failure pressure of a laboratory-scaled specimen can be one order of magnitude higher than that of a full-scale structure, different damage propagation and arrest are expected in a full-scale structure.

Introduction

STRUCTURAL integrity is one of the important considerations in the design of an aircraft fuselage. The concept of damage tolerance, defined as the ability of a structure/material to perform given a particular requirement with damage present, provides some guidelines to ensure structural integrity in design. This design philosophy was adopted in the mid-1970s by the U.S. Air Force.[1] In the damage tolerant design philosophy, the existence of flaws due to manufacturing and in-service conditions is acknowledged. Such damage can then grow under loading. When damage reaches a critical size, the structure loses its structural integrity, which leads to catastrophic failure. The aim of damage tolerant design is to prevent this from occurring.

Related to the damage tolerant philosophy is the concept of damage arrest. This is defined as the ability of a structure or material to arrest a propagating damage before such damage causes catastrophic failure. Damage arrest can be accomplished by a variety of schemes. One such scheme is to attach stiffening structural elements such as tear straps to the main structure. Tear straps or stiffening bands modify the local stress and strain fields in the stiffened region, constrain further opening of the crack boundary, and reduce the stress intensity at the crack tip. Much work in this area has been done on metallic structures.[2–5] With an increasing use of advanced composites in aircraft design and a potential use of such materials in primary aerospace structures such as an aircraft fuselage,[6,7] there is a need to understand the mechanisms of damage propagation and arrest in composite structures.

Some of the earlier work on damage arrest in composites done in the mid-1970s (Refs. 8 and 9) considered the case of through-thickness damage. It is recognized that through-cracks do not represent realistic damage states for composite structures in service. However, a through-crack (a slit) is a well-defined damage state and was used in such preliminary studies to determine the operative mechanisms in damage arrest. In this early work, two different arrest schemes were proposed: 1) the use of buffer strips and 2) the use of stiffening strips.

Buffer strips are layers of different material(s), usually of lower stiffness but higher toughness than the base material. These strips are placed at certain locations to replace the base material. This arrest scheme was explored experimentally in Refs. 8 and 9, and it was observed that arrest was dependent upon the initial flaw size as arrest was not accomplished in panels with small initial flaw size. Significant delamination was also observed in the failed specimens. It was also found that the use of buffer strips in the base laminates can reduce the strength of the structure significantly. In summary, arrest could not be achieved in all cases using this scheme.

Another way to try to arrest the propagating damage in composites is to use stiffening strips.[10,11] In this concept, the base material is unaffected. The stiffening strips, which can be made of different material(s), can be introduced on the top or bottom surface of the base material or even interleaved within a laminate. This arrest concept in composite structures is very similar to the use of crack arrest members in metallic structures where crack arrestors or tear straps are attached to the base structure.[2,3]

The current work builds on the results and understanding attained in previous experimental work to achieve a better understanding of the issues of damage arrest in composite structures, particularly pressurized cylinders, and the mechanisms associated with such. A quick review of previous key results is therefore important.

Previous Key Results

In the previous experimental work on damage arrest in pressurized composite cylinders,[12–14] only the effects of the hoop stiffening bands on damage propagation were studied. The cylindrical specimens investigated had a diameter of 305 mm (12 in.) and were 750 mm (30 in.) long. Two different types of graphite/epoxy materials with the same brand of epoxy were investigated: a satin-weave fabric material (AW370-5H/3501-6) and a unidirectional tape material (AS4/3501-6). The stiffeners were cocured with the cylinders and were constructed from one material only (the unidirectional tape AS4/3501-6). The stiffening bands were placed approximately 203 mm (8 in.) apart, so that their influence on the stress/strain fields

Received Feb. 6, 1996; revision received Aug. 17, 1996; accepted for publication Sept. 18, 1996; also published in *AIAA Journal on Disc*, Volume 2, Number 1.

*Ph.D. Candidate, Technology Laboratory for Advanced Composites, Department of Aeronautics and Astronautics; currently Consultant/Associate, McKinsey and Co. Management Consulting Firm, Midplaza 2 Building, 18th Floor, JL. Jenderal Sudiman Kav. 10-11, Jakarta 10220, Indonesia.

†Undergraduate Researcher, Technology Laboratory for Advanced Composites, Department of Aeronautics and Astronautics; currently Product Development Engineer, Ford Motor Company, P.O. Box 2053, Dearborn, MI 48121.

‡Professor and MacVicar Faculty Fellow, Technology Laboratory for Advanced Composites, Department of Aeronautics and Astronautics, 77 Massachusetts Avenue. Associate Fellow AIAA.

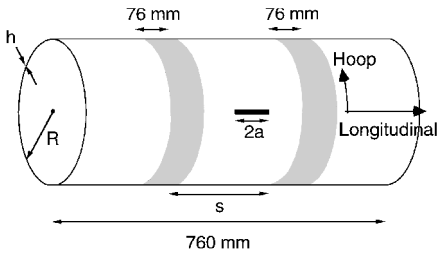

Fig. 1 Geometry of circumferentially stiffened cylinder used in previous work[13,14]: $R = 152$ mm, $h = 1.4$ mm, and $s = 203$ mm. Note: not to scale.

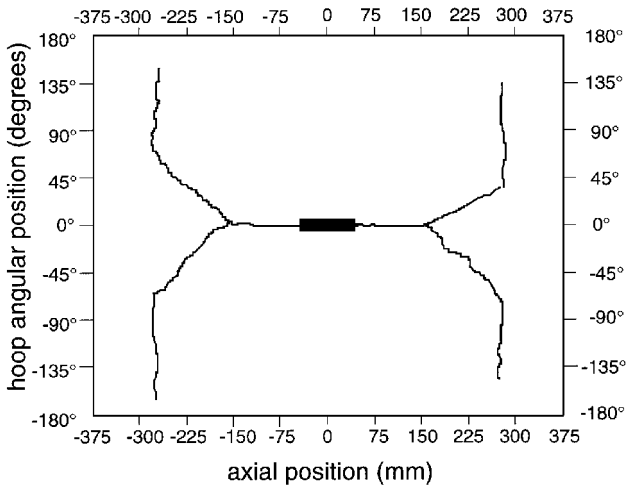

Fig. 2 Typical fracture path for an unstiffened fabric cylinder.

near the slit tip was negligible (the so-called noninteracting case). The stacking sequences studied were quasi-isotropic $(0/45)_s$ and $[90/0/\pm 45]_s$ and structurally anisotropic $[\pm 45/0]_s$ and $[\pm 45/90]_s$ (parentheses indicate fabric and brackets indicate unidirectional material). Note that the zero degree fiber direction is in the hoop direction of the cylinder. Typical cylinder geometry studied in these previous works is shown in Fig. 1. Each stiffened cylinder was internally pressurized to failure using nitrogen gas.

The two types of materials studied exhibited different fracture behavior.[13,14] The fracture of fabric cylinders tended to be relatively clean and so damage propagation could be easily traced from each fractured specimen. The tape cylinders, on the other hand, fractured into many different pieces, making it harder to identify the propagation path. Therefore, the discussion of the cylinder fracture path that follows is based mainly on the fabric cylinders. To present the fracture paths with clarity, it is imagined that the cylinder is cut along the longitudinal direction at an angular location exactly 180 deg from the slit and then rolled flat. The slit is now located at the center of the drawing (at the 0-deg angular location) as in Fig. 2. All fracture paths in this paper are presented in this format.

For the unstiffened cylinders, damage initially propagates in the longitudinal direction in a relatively self-similar way. It then bifurcates and branches into two distinct parts at approximately 200 mm from the endcaps as depicted in Fig. 2 (Refs. 12 and 13). This is different from what is observed in the stiffened cases where damage that initially propagates in the longitudinal direction can change its propagation path to the hoop direction as it approaches the edge of the stiffened regions given that enough stiffening is provided (see Fig. 3). It was suggested that the stiffener effectiveness be scaled by the number of stiffener layers.[14]

The cylinder fracture behavior shown in Fig. 2 is very different from what was observed experimentally in a stiffened composite panel containing a slit.[11] For the same stiffener configuration (same material and number of layers), stiffening layers had practically no effects on the subsequent damage propagation in a flat plate. Damage practically did not recognize the presence of the stiffening bands and continued its propagation perpendicular to the loading through the stiffeners, inducing delamination and stiffener debonds.

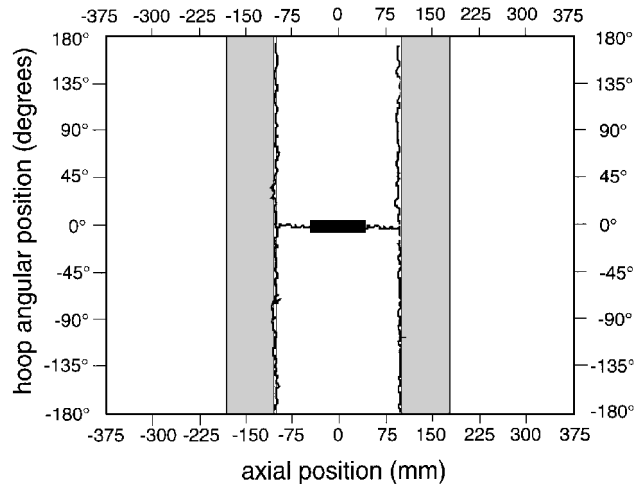

Fig. 3 Typical fracture path for fabric cylinder stiffened in the hoop direction in which enough degree of stiffening is provided.

For the same stacking sequence and stiffener configuration, cylinder and flat plate differ in two ways. One, the loading condition is different as the cylinder is loaded by internal pressure whereas the plate is loaded only in membrane tension. This leads to a phenomenon in the cylinder known as bulging, which is defined as the out-of-plane deformation of the crack region that is induced by a combination of internal pressure and geometric coupling between the membrane and bending actions in a shell structure. Bulging results in an intensification of stress at the slit tip in a cracked shell.[15] The second difference is stiffener curvature as the hoop stiffener in a cylinder is curved while that in a plate is flat. These two factors contribute to the observed differences in the fracture paths of the two structures. Because of these two effects (loading and stiffener curvature), bending behaviors of the two structures are different as the slit propagates and approaches the stiffeners. Although bending can also exist in a stiffened plate due to bending-stretching coupling induced by the unsymmetric nature of the stiffened plate, considerably more bending exists in a cylinder particularly due to pressure loading and curvature effects. It was then postulated that bending stiffness is one of the important factors in determining stiffener effectiveness to induce damage redirection[14] as an increase in bending stiffness has a large effect on the stress and strain field ahead of a propagating damage.

Using such a physical insight, a nondimensional containment ratio was proposed[14]:

$$C = (2a/R)(D_s/D_u) \tag{1}$$

where $2a$ is the slit size, R is the cylinder radius, and D_s and D_u are the bending stiffnesses of the stiffened and unstiffened regions, respectively. The driving force for damage propagation is inversely proportional to the initial slit size as a smaller slit results in a higher pressure at which damage propagation occurs. Because of this high driving energy, arrest or turning is more difficult to achieve in cylinders with small initial slits. As shown experimentally, stiffening bands in composite plates (which are locally flat) are not as effective as those in a cylinder (which are curved) in inducing damage bifurcation. Thus, the radius of curvature is important in determining stiffener effectiveness. Furthermore, as discussed previously, bending stiffness plays an important role in damage redirection, and that is quantified via the ratio of the bending stiffnesses of the stiffened and unstiffened regions. This containment parameter has been successfully applied to rank stiffener effectiveness in some structurally anisotropic cylinders.[14]

In summary, it has been shown experimentally that damage bifurcation in a composite cylinder can be induced by the reinforcement in the hoop direction. For the case in which bifurcation occurs, damage continues its propagation in the hoop direction and cylinder failure process continues in that direction during final rupture. Complete arrest of damage propagation was not accomplished and has not been explored further in the previous experimental investigations.

Therefore, there is a need to experimentally explore the possibility of complete arrest of damage in pressurized composite cylinders.

Objectives

Based on the identified needs, the objective of the present investigation is to experimentally investigate the influence of longitudinal reinforcements in the propagation of damage in pressurized composite cylinders. In particular, the combined effects of longitudinal and hoop stiffeners on the nature of damage propagation are of interest with the overall goal of achieving complete arrest in such structures. It is important to note that a cylindrical structure containing both longitudinal and hoop stiffening bands actually resembles an actual aircraft fuselage structure where tear straps are usually placed under the frames (hoop direction) and longerons (longitudinal direction).[16]

Approach

Five composite cylinders were manufactured from Hercules AW370-5H/3501-6 fabric graphite/epoxy material in a $(0/45)_s$ quasi-isotropic configuration. There are two reasons why the material system and quasi-isotropic configuration were used in the present study. First, the fracture paths of the cylinders constructed using this material system in this lay-up configuration were shown previously to be relatively clear and traceable. Traceable fracture paths are essential to study the possibility of damage arrest. The second reason is that the current study was built upon the results of a previous investigation in which the effects of hoop stiffening bands on damage propagation were explored for cylinders constructed using the same material system and stacking sequence.

All specimens were stiffened with the geometrical configuration shown in Fig. 4. The specimen geometry as depicted in Fig. 4 is based on the geometry used in previous work.[13,14] A total of four longitudinal stiffeners were placed symmetrically in each cylinder at 90-deg circumferential intervals. The notches in all cylinders were oriented in the longitudinal direction. Only one slit length, equal to 79 mm, was considered for all cases. There are several reasons for this. First, it was intended not to have an excessively high failure pressure (driving energy) during rupture, which would prevent the first bifurcation (damage redirection) from taking place. Previous work showed that bifurcation did occur for cylinders with a slit length of 79 mm (Refs. 12 and 13). Second, it was intended that the interaction between the stiffening bands and the stress fields near the initial slit tips be minimal. The distance between the two stiffeners was 203 mm; therefore longer initial slit sizes might violate this criterion. Lastly, it was also intended to set the first nondimensional ratio in the proposed containment parameter[14] (the ratio between the slit size and the cylinder radius) constant for all cases studied here so that the effects of bending stiffness could be isolated.

The two stiffener lay-up configurations considered are shown in Fig. 5. The type A stiffener consists of alternating continuous and broken stiffeners in the longitudinal and hoop directions. This scheme was chosen to eliminate overlaps (additional material) at the locations where the two types of stiffeners meet. For example, the first layer of the hoop band was continuous, but the first layer of the longitudinal band was discontinuous. The scheme was then reversed in the subsequent layer (i.e., in the second layer, the longitudinal band was continuous whereas the hoop band was not). The type A stiffener was manufactured from the Hercules AS4/3501-6 graphite/epoxy unidirectional tape material with the fibers running parallel to the reinforcing direction. This material was chosen to be consistent with previous work.[13,14] In the type A stiffener, due to the material system used (unidirectional material) and the alternating continuous and broken stiffener layers, matrix cracking in and through the stiffener layers is a possible damage mode. This can lead to subsequent delamination.[17,18] Thus, matrix crack paths exist in the type A configuration. In contrast, the type B stiffener is one continuous checkerboard stiffener configuration with no layers overlapping and no discontinuous layers at the intersection. The material for the type B stiffener was chosen to be the same woven fabric as the base material (AW370-5H/3501-6). This stiffener configuration was chosen to eliminate matrix crack paths that have been shown to induce other damage modes such as delamination.[17,18] Since the stiffnesses in the longitudinal and hoop directions for fabric material are almost identical, the longitudinal and hoop stiffeners have roughly the same stiffness values.

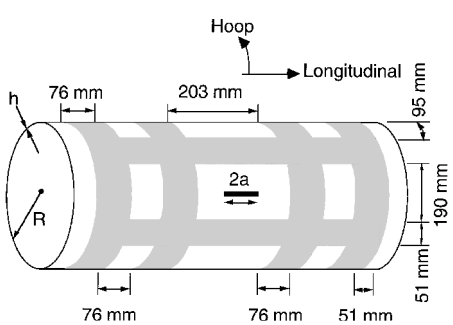

Fig. 4 Geometry of a typical stiffened cylinder in the present investigation: $R = 152$ mm, $h = 1.4$ mm, and $2a = 79$ mm. Note: not to scale.

Table 1 Stiffener configurations

Cylinder	Configuration type[a]	Number of plies in the hoop direction	Number of plies in the longitudinal direction
1	A	4 (0-deg tape)	8 (0-deg tape)
2	B	2 (0-deg fabric)	2 (0-deg fabric)
3	B	4 (0-deg fabric)	4 (0-deg fabric)
4	B	4 (45-deg fabric)	4 (45-deg fabric)
5	B[b]	4 (0-deg fabric)	8 (0-deg fabric)

[a]See Fig. 5. [b]Four additional 0-deg fabric layers in the longitudinal direction.

Table 2 Baseline properties of materials

Properties	AW370-5H/3501-6	AS4/3501-6
E_{11}, GPa	72.5	142
E_{22}, GPa	72.5	9.8
ν_{12}	0.059	0.30
G_{12}, GPa	4.43	6.0
t_{ply}, mm	0.350	0.134

Table 3 Bending stiffnesses of the stiffened cylinders tested

	Hoop direction		Longitudinal direction	
Cylinder	Value[a]	Ratio[b]	Value[a]	Ratio[b]
1	89	5.6	33	2.1
2	74	4.6	74	4.6
3	232	14.5	232	14.5
4	144	9.0	144	9.0
5	232	14.5	1047	65.4

[a]Bending stiffness in units of (GPa mm^3).
[b]Stiffened value/unstiffened value.

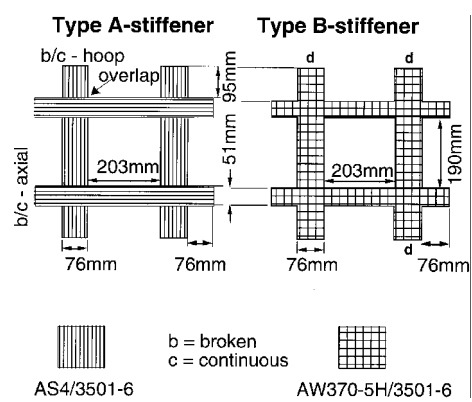

Fig. 5 Illustrations of the two different stiffener configurations utilized.

A complete description of the stiffener configurations is given in Table 1. These various configurations were utilized to consider the effect of different bending stiffness ratios (stiffened to unstiffened regions) in the hoop and longitudinal directions. These values, calculated using the material properties in Table 2 and with respect to the midplane of the base laminate, are given in Table 3. The bending

stiffness of the unstiffened region is 16 GPa mm^3 in both directions. The work was done in a progressive fashion such that results from earlier tests were utilized to determine configurations for later tests.

All cylinders were pressurized to failure using nitrogen gas inside a blast chamber. The fracture paths were obtained after the tests had been completed. The experimental details are given in the next section.

Experimental Procedure

All cylinders were laid up by hand on a cylindrical aluminum mandrel. The stiffeners were laid up on the external surface of each cylinder prior to cure. Additional stiffening bands were also placed in the hoop direction near the ends of each cylinder (see Fig. 4). Preliminary experiments showed that, in the presence of longitudinal stiffeners, there was a tendency for the cylinder cross section to be distorted after cure. A distorted cross section would cause difficulties in placing the cylinder on its endcaps and was therefore avoided here. Hence, these additional stiffeners were utilized to maintain the circular cross section of the cylinder during and after the cure process. All five cylinders were cured using the standard manufacturer's cure cycle of a 1-h flow stage at 116°C and a 2-h set stage at 177°C. This was performed under vacuum inside an autoclave under 0.59 MPa external pressure. After the cure had been completed, all cylinders were postcured in an oven at 177°C for 8 h without any external pressure. The resulting cylinder average wall thickness of 1.34 mm was within 5% of the nominal value of 1.40 mm.

Slits in all cylinders were cut using a 30,000-rpm rotary tool with a 25-mm diam and 0.6-mm-thick cutting blade mounted vertically on a milling machine arm. Slits were cut to the correct length and notched at the tips by hand using a small jeweler's saw. An even and smooth area away from the ply seams was chosen for the location of the slit. The length and width of each slit were 79 and 0.8 mm, respectively. Because of the destructive nature of the test, a 50 × 50 mm grid was drawn on the entire exterior surface of each cylinder with white paint. The grid squares were individually labeled to facilitate damage propagation trace.

Cylinder testing was accomplished via pressurization using bottled nitrogen and therefore required sealing of the cylinders. The cylinders were sealed at both ends by bonding them in grooves cut into aluminum endcaps, 330 mm (13 in.) in diameter and 25 mm (1 in.) thick. One of the endcaps had a lead for the nitrogen gas. An internal rubber bladder, made of 0.8-mm-thick gum rubber, was placed inside the cylinder to contain the pressurizing gas. The cylinders were attached to a pressure transducer so that internal pressure through the test and at failure could be recorded.

Cylinder testing was conducted in a blast chamber. A cylinder was placed horizontally on an iron channel in the center of the blast chamber. The cylinder, which rested on its endcaps, was oriented slit up so that the majority of the failure path would not be constrained by the channel. The ends of the cylinder were not fixed to the channel and no restrictions were made on longitudinal movement or expansion of the cylinder. Cylinder pressurization was controlled manually with the use of a pressure regulator attached directly to a nitrogen tank at an approximate rate of 0.4 MPa/min. The pressurization rate was monitored during the test via a dial gauge and a chart recording of the pressure transducer output. Cylinder pressure data were collected at 0.5-s intervals.

Photographs were taken of all specimens tested to record failure modes and fracture paths. Drawings of fracture paths were made for all cylinders to identify the primary fracture path as well as to determine the effects of stiffening bands on damage propagation.

Failure Results

Before considering damage paths, it is first important to consider the failure pressures to assure that the initial conditions for damage propagation were the same for all cases.

Failure Pressure

Failure of a pressurized composite cylinder containing a longitudinal slit can be predicted using a methodology based on the Mar-Lin composite fracture correlation[19] modified for curvature effects.[15] The resulting formula for predicted failure pressure is[12,13]

$$p_{\text{pred}} = \frac{t}{R}\frac{H_c(2a)^{-0.28}}{[1+0.317\lambda^2]^{0.5}} \tag{2}$$

where t is the cylinder thickness, H_c is the composite fracture parameter,[20] which is laminate specific and obtained experimentally, and λ is the nondimensional crack length defined as[15]

$$\lambda = (a/\sqrt{Rt})\sqrt[4]{12(1-\nu^2)} \tag{3}$$

where ν is the Poisson's ratio of the material. For the AW370-5H/3501-6 $(0/45)_s$ laminate, H_c has been experimentally measured to be 698 MPa (mm)$^{0.28}$ (Ref. 21).

The experimental failure pressures of the cylinders are tabulated in Table 4. The predicted failure pressures were computed using both the nominal wall thickness of 1.4 mm and radius of 152 mm and the average measured wall thickness of 1.34 mm and radius of 153 mm. This yields predicted failure pressures of 645 and 603 kPa, repspectively. The agreement between the predicted and experimental failure pressure is very good. This good agreement and the small deviation in actual measured values show the consistency of the test specimens in the present study with those manufactured in the previous work and that the specimens in this work can be directly compared. It also shows that the stiffeners were indeed noninteracting with the stress fields near the slit prior to damage propagation.

Fracture Paths

Only the descriptions of the fracture paths are presented in this section with a discussion presented in the following section. All fracture paths are presented using the same format used in Fig. 2 in which it is imagined that the cylinder is cut along the longitudinal direction at an angular location exactly 180 deg from the slit and rolled flat. Therefore, the initial slit is now located at the center of the drawing. The longitudinal slit is represented by a thick solid line, the damage path is represented by thinner solid lines, and delamination and stiffener debonds are represented by shaded regions.

The fracture path of cylinder 1 is shown in Fig. 6. Damage initially propagated from each slit tip in the longitudinal direction and then bifurcated and turned 90 deg very close to the edge of the hoop stiffeners. After bifurcation, damage that had split into four distinct paths continued to propagate in the hoop direction and induced other damage modes (stiffener debonds) near the junction between the

Table 4 Failure data for all cylinders

Cylinder	Failure pressure, kPa
1	579
2	566
3	551
4	612
5	607

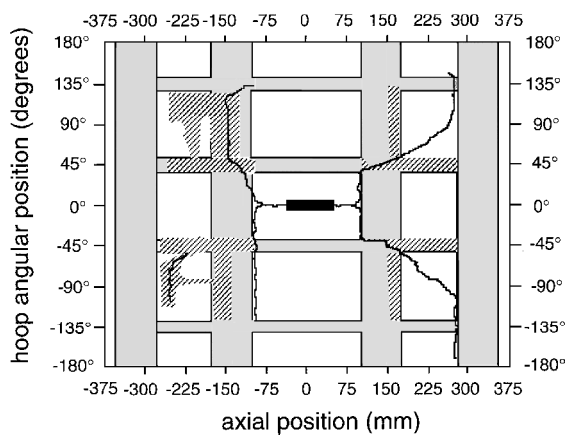

Fig. 6 Fracture path of cylinder 1 stiffened with four layers of 0-deg tape (hoop) and eight layers of 0-deg tape (longitudinal).

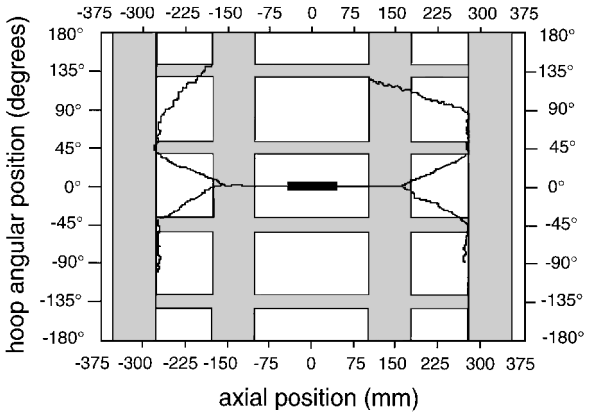

Fig. 7 Fracture path of cylinder 2 stiffened with two layers of continuous (type B) 0-deg fabric layers.

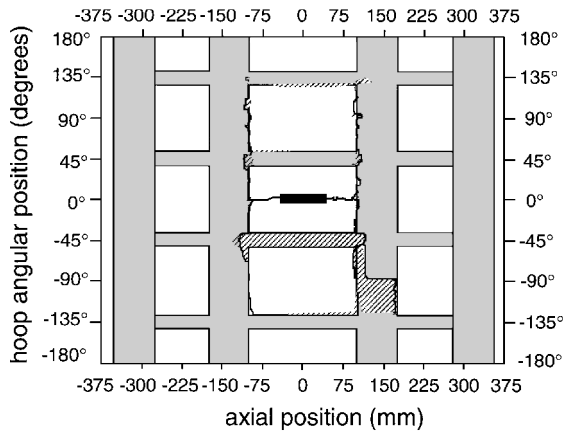

Fig. 8 Fracture path of cylinder 3 stiffened with four layers of continuous (type B) 0-deg fabric layers.

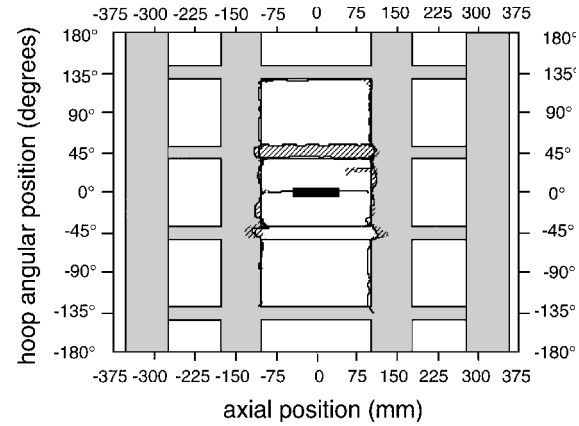

Fig. 9 Fracture path of cylinder 4 stiffened with four layers of continuous (type B) 45-deg fabric layers.

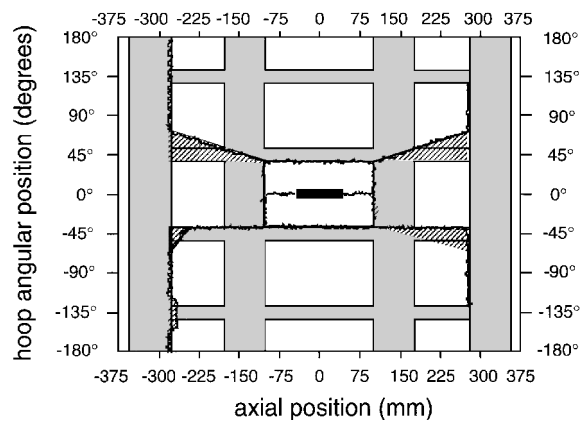

Fig. 10 Fracture path of cylinder 5 stiffened with four layers of continuous (type B) 0-deg fabric layers and four additional continuous 0-deg fabric layers in the longitudinal direction.

longitudinal and hoop stiffeners and delamination in the unstiffened regions. Some damage turning can also be seen in the fracture path at this junction. The damage was arrested by the next set of longitudinal stiffeners at an angular location approximately 135 deg from the slit.

The fracture path of cylinder 2 is shown in Fig. 7. Damage also initially propagated in the longitudinal direction. However, as the damage continued to propagate, the hoop stiffener did not have a discernible effect as damage propagation continued in the longitudinal direction until it branched into two parts within the first set of hoop stiffeners at an approximate angle of 40–50 deg from the longitudinal axis. The bifurcated damage maintained this angular direction and then completely turned 90 deg at the second set of hoop stiffeners. These additional hoop stiffeners were intended to maintain the cross section of the cylinder after cure and were placed close to the endcaps (at an approximate distance of 50 mm). The overall fracture path was relatively clean with little delamination observed and was very similar to that of an unstiffened cylinder. Thus, for this particular case, even the first set of hoop stiffeners was not effective in inducing the first bifurcation.

In cylinder 3, which was stiffened with four layers of 0-deg continuous fabric layers, damage was turned as it reached the edge of the hoop stiffeners. It then continued its propagation in the hoop direction, fracturing and delaminating one set of the longitudinal stiffening bands during its progression. Some further debonding was also observed in the hoop stiffener far from the slit region as depicted in Fig. 8. A similar fracture path was observed in cylinder 4, which was stiffened with four continuous layers of 45-deg fabric layers as shown in Fig. 9. Some fracture of the longitudinal stiffeners was also observed while damage propagated across the region. As in cylinder 1, damage was arrested by the next set of longitudinal stiffeners.

A slightly different fracture behavior was observed when more reinforcement in the longitudinal direction was provided in cylinder 5 as shown in Fig. 10. This cylinder was stiffened with four layers of continuous 0-deg fabric and was further reinforced with four additional 0-deg fabric layers in the longitudinal direction. As in cylinders 3 and 4, damage was successfully turned by the hoop stiffeners. It then continued its propagation in the hoop direction, reaching the edge of the first set of longitudinal stiffeners where redirection to longitudinal propagation was observed. However, some of the bifurcated damage turned and continued to propagate at an angle of approximately 40 deg, inducing stiffener debonds, fracturing the hoop stiffeners, and delaminating the base cylinder along the way. The damage was totally arrested on one side of the second set of longitudinal stiffeners.

Discussion

In all but one case, the first set of hoop stiffeners was effective in inducing branching as damage turned and propagated near the edge of the hoop stiffeners. However, no branching was observed in the fracture path at the first set of hoop stiffeners of cylinder 2. Using the proposed nondimensional containment ratio shown in Eq. (1), only the bending stiffness ratio needs to be considered since the slit size and the radius of all cylinders are the same. The bending stiffnesses of the stiffened and unstiffened regions in the hoop direction are shown in Table 3. Note that cylinder 2 was stiffened with two layers of 0-deg fabric. Although the hoop stiffeners in cylinder 2 were actually thicker than those in cylinder 1 (0.70 mm for cylinder 2 vs 0.54 mm for cylinder 1), the in-plane stiffness of a fabric material is only roughly one-half of the value for unidirectional tape material. Thus, cylinder 2 has the lowest value of bending stiffness ratio, which means that it also has the lowest value of containment ratio. The inability of the stiffening band in cylinder 2 has therefore been explained using the proposed containment parameter. When more stiffening layers were added to the cylinder, this ratio increased and damage bifurcation took place as can be seen in cylinders 3–5.

In cases where the first set of hoop stiffeners was effective in inducing damage redirection, damage continued its propagation in

the hoop direction, generally cleanly breaking the longitudinal stiffening bands along the way. These can be seen clearly in the fracture paths of cylinders 1, 3, and 4 shown in Figs. 6, 8, and 9, respectively. Cylinder 1, which was reinforced with the type A stiffener, suffered significant secondary damage in the form of delamination and stiffener debonding near the locations where the longitudinal and hoop reinforcements meet. Thus, although damage may appear to have been diverted/turned in this case, it is more likely that it just found an easier path (via matrix cracking and associated delamination) along which to propagate.

In cylinders 3–5, matrix crack initiation at the location where the longitudinal and hoop stiffeners meet was eliminated through the use of the type B stiffener configuration. This also reduced the potential for the associated delamination. However, eliminating this matrix crack path did not significantly increase the effectiveness of the longitudinal stiffeners closest to the slit in arresting damage as can be seen in Figs. 8 and 9. Damage continued its propagation across the first set of longitudinal stiffeners but was then arrested at the next longitudinal stiffeners, which were at angular locations of approximately $\pm$135 deg from the slit. Note that redirection by the first set of longitudinal stiffeners was observed in cylinder 5 as depicted in Fig. 10. Such a cylinder contained more reinforcement in the longitudinal direction (up to eight layers of 0-deg fabric). Despite the observed turning, damage that now had split into four independent paths continued to propagate and induced a considerable amount of secondary damage modes such as stiffener debonding, hoop and longitudinal stiffener breakage, as well as delamination of the unstiffened (base) region. One set of the bifurcated damage continued its propagation due to a separation of one of the endcaps from the cylinder during rupture. The other set of bifurcated damage was arrested at the next set of longitudinal stiffeners located at angular locations of approximately $\pm$135 deg from the slit as in cylinders 1, 3, and 4.

To understand this observed phenomenon, the magnitudes of the longitudinal bending stiffnesses of the stiffened and unstiffened regions are reexamined. These are tabulated in Table 3. The bending stiffness ratios in the longitudinal direction range from 2.1 (for cylinder 1) to 65.4 (for cylinder 5). In cylinders 1, 3, and 4, damage was able to continue its propagation in the hoop direction through the first set of longitudinal stiffeners. In cylinder 5, with the highest longitudinal bending stiffness ratio, damage did turn as it propagated in the hoopwise direction and met the first set of longitudinal stiffeners. However, even in this case, damage was not completely arrested at the first set of stiffeners and continued its propagation. Therefore, as shown experimentally, the longitudinal stiffening bands were not as effective in arresting damage as the hoop stiffeners. This has been confirmed analytically by Duncan and Sanders.[22] The geometrical parameters in their analytical solution that determines the stiffener effectiveness are the stiffener curvature and the thickness of the stiffener. It is shown that, under identical loading and stiffener configuration, the hoop stiffener in a cylinder, which has roughly the same radius of curvature as the cylinder, is more effective in reducing the stress intensity factor than the stiffener in a flat plate (with no curvature). Since the longitudinal stiffening bands in a cylinder are similar to those in a plate and are locally flat, the reduced effectiveness of the longitudinal stiffeners is therefore expected.

In considering the relative effectiveness of hoop and longitudinal stiffeners to arrest/redirect damage, it is important to consider the driving force during different stages of damage propagation. The overall damage propagation can be separated into two stages: 1) before the first bifurcation takes place in which damage turns from the longitudinal to the hoop direction and 2) after the first bifurcation in which the bifurcated damage continues its propagation in the hoop direction. In the first stage, damage propagates in a relatively self-similar way with the cylinder hoop stress as the scaling/driving parameter. This stage of damage propagation is the bulging phenomenon.[12,15] The second stage of damage propagation is caused by the flapping phenomenon induced by internal pressure[23] as depicted in Fig. 11.

The existence of two different driving forces that exist as damage propagates is proposed as one of the reasons why damage was not arrested by the first set of longitudinal stiffeners that were closest to the slit. To determine the proper scaling/driving parameter after flapping occurs, a first-cut engineering model is proposed based on

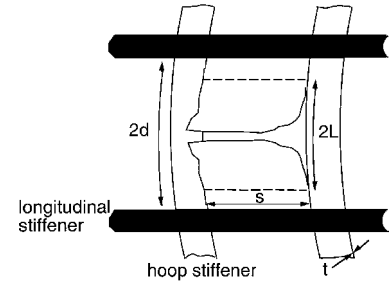

Fig. 11 Illustration of flapping induced by crack bifurcation in a pressurized cylinder.

dimensional argument. The cylindrical panel considered is shown in Fig. 11. In the panel considered, the initial damage is assumed to have bifurcated and split into four distinct parts. By modeling this phenomenon as the bending of a cantilevered plate under uniform pressure loading, the moment taken at the tip of the damage can be shown to be proportional to the pressure p and the distance L the damage has run in the hoop direction:

$$M \propto pL^2 \tag{4}$$

When the damage tip reaches the longitudinal stiffeners, this flapping distance is proportional to the spacing of the longitudinal stiffener denoted by $2d$ in Fig. 11. Therefore, Eq. (4) can be rewritten as

$$M \propto pd^2 \tag{5}$$

Based on elementary beam/plate theory, the bending stress can be shown to be

$$\sigma_b \propto My/I \tag{6}$$

where y is the distance from the neutral axis of the cylinder and I is the area moment of inertia with respect to the neutral axis. By substituting Eq. (5) into Eq. (6) and noting that y is proportional to the thickness t and I is proportional to the cube of the thickness, one can express the bending stress as

$$\sigma_b \propto p(d/t)^2 \tag{7}$$

with the key parameters thus being the pressure, the longitudinal stiffener spacing, and the base cylinder thickness. Also note that as flapping occurs, the driving force (pressure) decreases due to bending of the crack face, which allows the pressurizing gas to leave the cylinder. This is believed to be the reason for the observed damage arrest by the next set of longitudinal stiffeners located at angular locations of $\pm$135 deg as seen in the fracture paths of cylinders 1, 3, and 4.

Implications

There are two separate physical problems that influence damage propagation and arrest in pressurized composite cylinders. The first physical phenomenon is the bulging phenomenon, which governs the damage propagation before the first bifurcation. The scaling/driving parameter for this phenomenon is the hoop stress, which involves the pressure, the cylinder radius, and the cylinder thickness. The effects of bulging on different cylinder geometries depend on the cylinder radius and thickness and are accounted for in the failure prediction methodology.[12] The second physical problem that is important only after the first bifurcation has taken place is flapping. Flapping is governed by the bending stress shown in Eq. (7) and involves the pressure, the longitudinal stiffener spacing, and the cylinder thickness.

To illustrate the potential pitfalls in using a subscale specimen to study both damage propagation and arrest, consider a full-scale fuselage and a potential laboratory-scaled specimen to simulate such. The former is taken to have the same basic geometry as the fuselage of a Boeing 737 airplane with a radius of 2 m, thickness of 1.4 mm, and tear strap spacing in the longitudinal direction of 240 mm (Ref. 16). The latter has the same geometry as the test specimens in the present study (radius of 150 mm, thickness of 1.4 mm, hoop stiffener spacing of 203 mm, and longitudinal stiffener spacing of 190 mm). The ultimate design pressure in a Boeing 737 airplane is on the order of 110 kPa. Before bifurcation, the hoop stresses of

the two cylinders are the proper scaling parameters, and they are set equal. Hence, to satisfy this criterion, the smaller cylinder must be pressurized up to approximately 1500 kPa. After bifurcation has taken place, the scaling/driving parameter of interest is the bending stress given by Eq. (7), which depends on the pressure at rupture, the longitudinal stiffener spacing, and the wall thickness. Note that the longitudinal stiffener spacings of these two cylinders are almost equal. Using Eq. (7), it can be shown that the magnitude of the bending stress in the smaller cylinder is approximately nine times that of the larger cylinder (almost one order of magnitude difference). Therefore, from this comparison, it is clear that it may not be possible to properly simulate/scale both the bulging and flapping phenomena in an experiment on a subscale specimen as different scaling parameters govern the two phenomena. Thus, this is one of the reasons why arrest by the longitudinal stiffener is more difficult to accomplish in a small-scale specimen.

The experiments performed in the present study used a flat tear strap configuration. In an actual fuselage, stiffening elements of other geometry (such as top hat and Z-section stiffeners) are bonded to or placed on top of the flat tear straps.[16] These additional stiffening members are used to provide additional membrane and bending stiffnesses against bending and buckling of the fuselage structure. However, their effects on the damage propagation in such a structure are unclear at this time and should be subject for future study.

Conclusions

The combined effects of longitudinal and hoop stiffeners on the damage propagation in pressurized composite cylinders have been investigated experimentally. It has been shown that the stiffening elements in the hoop direction are more effective in redirecting damage than those in the longitudinal direction. Damage continues its propagation in the hoop direction despite the presence of longitudinal stiffeners. This behavior is attributed to two reasons. First, it has been shown from a previous analytical solution that stiffener curvature plays a significant role in influencing the stress fields near the slit tips (i.e., the higher the curvature, the more effective the stiffener). Since the stiffening band in the longitudinal direction has zero curvature locally, more reinforcement will be needed in the longitudinal direction than in the hoop direction. The second reason is the size effects, which cause the scaling parameter for damage growth to be different depending on the stages of damage progression. At the later stage of damage growth (after bifurcation has taken place), the bending stress shown in Eq. (7) becomes the proper scaling parameter rather than the membrane hoop stress. Since the smaller cylinder fails at a higher pressure than the larger one, the condition in the smaller specimen is therefore much more severe than that in the larger one. Even additional reinforcements in the longitudinal direction in a laboratory-scaled specimen are ineffective and total arrest is more difficult to accomplish. Therefore, although the full-scale structure and the subscale specimen are geometrically scaled for initial damage and driving force (hoop stress), the condition in the subscale specimen during damage propagation after bifurcation is much more severe than that in a full-scale structure since the driving forces change during damage propagation. Total arrest in a subscale specimen is therefore much more difficult to achieve. The existence of different scaling parameters for damage propagation in the longitudinal and hoop directions makes it difficult, if at all possible, to completely model the damage propagation and arrest characteristics of a full-scale pressurized cylinder such as a fuselage with a smaller-sized specimen.

Acknowledgments

This work was supported by the Aircraft Structures Branch of NASA Langley Research Center under Grant NAG1-991. Many collaborations with the Contract Monitor, James H. Starnes Jr., are gratefully acknowledged.

References

[1]Anon., "Military Specification: Airplane Damage Tolerance Requirements," U.S. Air Force, MIL-A-83444, Wright–Patterson AFB, Dayton, OH, July 1974.

[2]Swift, T., and Wang, D. Y., "Damage Tolerant Design Analysis Methods and Test Verification of Fuselage Structure," *Air Force Conference on Fatigue and Fracture*, U.S. Air Force Flight Dynamics Lab., AFFDL-TR-70-144, Wright–Patterson AFB, Dayton, OH, 1962, pp. 653–683.

[3]Swift, T., "Development of the Fail-Safe Design Features of the DC-10," *Damage Tolerance of Aircraft Structures*, American Society for Testing and Materials, ASTM STP 486, Philadelphia, PA, 1971, pp. 162–214.

[4]Kanninen, M. F., Sampath, S. G., and Popelar, C., "Steady-State Crack Propagation in Pressurized Pipelines Without Backfill," *Journal of Pressure Vessel Technology*, Vol. 98, No. 1, 1976, pp. 56–65.

[5]McGuire, P. A., Sampath, S. G., Popelar, C. H., and Kanninen, M., "A Theoretical Model for Crack Propagation and Crack Arrest in Pressurized Pipelines," *Crack Arrest Methodology and Applications*, American Society for Testing and Materials, ASTM STP 711, Philadelphia, PA, 1980, pp. 341–357.

[6]Ilcewicz, L. B., Smith, P. J., and Horton, R. E., "Advanced Composite Fuselage Technology," *3rd NASA Advanced Composites Technology Conference* (Long Beach, CA), NASA CP-3178, Pt. 1, June 1992, pp. 97–156.

[7]Smith, P. J., Thompson, L. W., and Wilson, R. D., "Development of Pressure Containment and Damage Tolerance Technology for Composite Fuselage Structures in Large Transport Aircraft," NASA CR-3996, July 1986.

[8]Sendeckyj, G. P., "Concepts for Crack Arrestment in Composites," *Fracture Mechanics of Composites*, American Society for Testing and Materials, ASTM STP 593, Philadelphia, PA, 1975, pp. 215–226.

[9]Bhatia, N. M., and Varette, R. M., "Crack Arrest of Laminated Composites," *Fracture Mechanics of Composites*, American Society for Testing and Materials, ASTM STP 593, Philadelphia, PA, 1975, pp. 200–214.

[10]Jozavi, H., Dupuis, C. W., and Sancaktar, E., "An Investigation of the Fracture Behavior of a Composite Crack Arrestor," *Journal of Composite Materials*, Vol. 22, No. 5, 1988, pp. 427–446.

[11]Sawicki, A. J., Graves, M. J., and Lagace, P. A., "Failure of Graphite/Epoxy Panels with Stiffening Strips," *Composite Materials: Fatigue and Fracture-Fourth Volume*, American Society for Testing and Materials, ASTM STP 1156, Philadelphia, PA, 1993, pp. 5–34.

[12]Graves, M. J., and Lagace, P. A., "Damage Tolerance of Composite Cylinders," *Composite Structures*, Vol. 4, No. 1, 1985, pp. 75–91.

[13]Graves, M. J., and Sawicki, A. J., "The Failure of Integrally Stiffened Graphite/Epoxy Cylinders," *Composite Structures*, Vol. 27, No. 3, 1994, pp. 269–282.

[14]Ranniger, C. U., Lagace, P. A., and Graves, M. J., "Damage Tolerance and Arrest Characteristics of Pressurized Graphite/Epoxy Tape Cylinders," *Composite Materials: Fatigue and Fracture-Fifth Volume*, American Society for Testing and Materials, ASTM STP 1230, Philadelphia, PA, 1995, pp. 407–426.

[15]Folias, E. S., "On the Predictions of Catastrophic Failures in Pressurized Vessels," *Prospects of Fracture Mechanics*, edited by G. C. Sih, H. C. van Elst, and D. Broek, Nordhoff International, Leyden, The Netherlands, 1974, pp. 405–418.

[16]Niu, C. Y. M., *Airframe Structural Design*, Conmilit Press, Ltd., Hong Kong, 1988, pp. 376–429.

[17]Lagace, P. A., Bhat, N. V., and Gundogdu, A., "Response of Notched Graphite/Epoxy and Graphite/PEEK Systems," *Composite Materials: Fatigue and Fracture-Fourth Volume*, American Society for Testing and Materials, ASTM 1156, Philadelphia, PA, 1993, pp. 55–71.

[18]Simonds, R. A., and Stinchcomb, W. W., "Response of Notched AS4/PEEK Laminates to Tension/Compression Loading," *Advances in Thermoplastic Matrix Composite Materials*, American Society for Testing and Materials, ASTM STP 1044, Philadelphia, PA, 1989, pp. 133–145.

[19]Mar, J. W., and Lin, K. Y., "Fracture of Boron/Aluminum Composites with Discontinuities," *Journal of Composite Materials*, Vol. 11, Oct. 1977, pp. 405–421.

[20]Lagace, P. A., "Notch Sensitivity and Stacking Sequence of Laminated Composites," *Composite Materials: Testing and Design (7th Conference)*, American Society for Testing and Materials, ASTM STP 893, Philadelphia, PA, 1986, pp. 161–176.

[21]Ranniger, C. U., "Effect of Cylinder Diameter on the Damage Tolerance of Graphite/Epoxy Cylinders with Longitudinal Notches," Massachusetts Inst. of Technology, TELAC Rept. 91-10, Cambridge, MA, May 1991.

[22]Duncan, M. E., and Sanders, J. L., "The Effect of a Circumferential Stiffener on the Stress in a Pressurized Cylindrical Shell with a Longitudinal Crack," *International Journal of Fracture Mechanics*, Vol. 5, No. 2, 1969, pp. 133–155.

[23]Swift, T., "Damage Tolerance in Pressurized Fuselages," *Proceeding of the 14th Symposium of International Committee on Aeronautical Fatigue (ICAF)* (Ottawa, CA), Cradley Heath, Warley, West Midlands, England, UK, 1987, pp. 1–78.